EEET ECOLOGICAL ENGINEERING & ENVIRONMENTAL TECHNOLOGY

Ecological Engineering & Environmental Technology, 2026, 27(12), 1–24
https://doi.org/10.12912/27197050/226436
ISSN 2719–7050, License CC-BY 4.0

Received: 2026.07.08
Accepted: 2026.10.16
Published: 2026.11.02

Dynamic rainfall and urban landscape adaptive capacity for flood resilience in Makassar City, Indonesia

Junardin Djamaluddin[1], Hazairin Zubair[2], Tigin Dariati[3], Eymal Bahsar Demmallino[1*], Hari Iswoyo[3], Samsu Arif[4]

[1] Environmental Science Study Program, The Graduate School, Hasanuddin University, Makassar, Indonesia
[2] Department of Soil Science, Faculty of Agriculture, Hasanuddin University, Makassar, Indonesia
[3] Department of Agrotechnology, Faculty of Agriculture, Hasanuddin University, Makassar, Indonesia
[4] Department of Geophysics, Faculty of Mathematics and Natural Sciences, Hasanuddin University, Makassar, Indonesia
* Corresponding author's e-mail: demmallino2019@gmail.com

ABSTRACT

Urban flooding in Makassar City is influenced by rainfall variability, urban development, and limited landscape capacity to regulate stormwater. This study applied a pressure–sensitivity–adaptive capacity (PSAC) framework to spatially assess the interaction between hydrological pressure, flood susceptibility, and landscape adaptive capacity. A descriptive quantitative approach was employed using secondary rainfall data for 2015–2024 from the Indonesian Meteorological, Climatological and Geophysical Agency (BMKG), official flood-susceptibility data from the Regional Disaster Management Agency (BPBD), spatial planning information, and Green Open Space (GOS) data. Rainfall dynamics were evaluated using annual and seasonal precipitation, wet-month frequency, and variability indicators, while flood susceptibility and GOS distribution were assessed through GIS-based spatial analysis. The results showed substantial rainfall variability during the study period, with monthly precipitation ranging from 42.7 to 612.4 mm and a coefficient of variation of 48.1%. High and very high flood-hazard classes covered 34.8% of the study area, while GOS accounted for only 12.42% of the urban area, below the 30% spatial planning benchmark. Furthermore, 41.2% of exposed assets were located within high and very high flood-hazard zones. The PSAC priority areas showed 78.6% spatial overlap with moderate-to-high BPBD flood-susceptibility zones, indicating substantial spatial consistency with the institutional reference dataset. The study demonstrates that integrating dynamic rainfall pressure, urban sensitivity, and landscape adaptive capacity provides a more comprehensive spatial basis for prioritizing flood adaptation and blue–green infrastructure interventions in tropical coastal cities.

Keywords: adaptive capacity; flood susceptibility; rainfall variability; green open space; PSAC framework

INTRODUCTION

Urban flooding has become one of the most significant environmental challenges affecting rapidly growing cities worldwide, particularly in tropical coastal regions where intense rainfall events coincide with accelerated urban expansion and land-use transformation. Climate variability has altered rainfall regimes by increasing the frequency and intensity of extreme precipitation, thereby intensifying surface runoff and overwhelming existing urban drainage systems. Simultaneously, rapid urbanization has increased impervious surface coverage, reduced infiltration capacity, and disrupted natural hydrological processes, contributing to flash floods, infrastructure damage, economic losses, and environmental degradation (Fletcher et al., 2024; Hathaway et al., 2024; Xiong & Yang, 2025; Bilgiç & Baba, 2023; Tang et al., 2024; McGrane, 2016; Kaiser

& Akter, 2025; Palacio-Aponte et al., 2022; Faccini et al., 2021). Consequently, flood management has increasingly shifted from conventional structural approaches toward integrated urban resilience strategies that consider hydrological processes, land-use dynamics, and ecosystem-based adaptation (Latief et al., 2025; Hasbi et al., 2025; Rahmawati et al., 2025; Tumpu et al., 2026; Syahriwati et al., 2025). Rainfall variability is a principal driver of urban flooding because precipitation directly influences runoff generation, peak discharge, and drainage-system performance. However, rainfall alone cannot fully explain flood occurrence, as flood impacts are also shaped by urban morphology, topography, drainage efficiency, and land-cover characteristics (Cruz et al., 2026; Ilmi et al., 2025; Guimarães et al., 2026; Bishikwabo et al., 2025; Posite et al., 2025; Wang et al., 2023; Xing et al., 2025). Accordingly, recent urban hydrology research recommends integrating rainfall analysis with spatial assessments of flood susceptibility and landscape characteristics to improve flood-risk interpretation and support adaptive urban planning (He et al., 2026; Miranda et al., 2023).

Makassar City, one of the fastest-growing metropolitan areas in eastern Indonesia, has experienced increasingly frequent urban flooding during the last decade. Population growth, expansion of residential and commercial areas, and the conversion of permeable land into impervious surfaces have reduced the city's natural capacity to absorb rainfall. Seasonal precipitation associated with the Asian–Australian monsoon frequently exceeds the capacity of existing drainage infrastructure, particularly during the November–March wet season, resulting in recurrent flooding across several urban districts. Previous studies in Makassar and other Indonesian cities have primarily examined rainfall characteristics, drainage performance, flood inundation mapping, or land-use change as independent determinants of flooding. Although these studies have improved understanding of flood mechanisms, they have rarely incorporated ecological adaptive capacity, particularly the contribution of green open space (GOS), into an integrated flood-resilience assessment (Yang et al., 2018; Ricart et al., 2022; Liao, 2014). Recent developments in urban resilience research emphasize the need for frameworks that simultaneously capture environmental pressure, urban sensitivity, and adaptive capacity. The pressure–sensitivity–adaptive capacity (PSAC) framework provides such a basis by conceptualizing rainfall dynamics as hydrological pressure, flood-prone landscapes as urban sensitivity, and Green Open Space as adaptive capacity through its contribution to infiltration, runoff regulation, local hydrological processes, and ecosystem resilience (Wang et al., 2024; Liu & Zhang, 2025; Kumareswaran & Jayasinghe, 2023; Cea & Costabile, 2022).

Although previous studies have increasingly integrated rainfall variability, GIS-based flood susceptibility mapping, and land-use characteristics, most approaches remain largely static or sequential, treating hydrological pressure, urban sensitivity, and ecological adaptation as separate analytical components. Quantitative applications that explicitly link long-term rainfall variability, flood susceptibility, and green open space distribution within a unified PSAC-based assessment remain limited, particularly for rapidly urbanizing tropical coastal cities such as Makassar. The scientific novelty of this study therefore lies not in the individual use of rainfall analysis, GIS, or the PSAC framework, but in their operational integration into a dynamic spatial assessment of urban flood resilience. Specifically, rainfall variability is conceptualized as a dynamic hydrological pressure, flood susceptibility and urban exposure as spatial expressions of urban sensitivity, and green open space and related landscape characteristics as measurable components of landscape adaptive capacity. This integration links temporal hydroclimatic pressure with spatial urban sensitivity and ecological adaptive capacity, thereby moving beyond conventional hazard mapping toward a more comprehensive interpretation of how these dimensions interact to produce heterogeneous flood-risk patterns. The framework is intended to provide a transferable analytical structure for rapidly urbanizing tropical coastal cities where rainfall variability, land-use transformation, and declining ecological capacity interact to generate recurrent flooding.

Despite considerable progress in urban flood research, an important knowledge gap remains regarding the integrated evaluation of rainfall dynamics, flood vulnerability, and adaptive landscape capacity within a single analytical framework. This study addresses that gap by applying the PSAC framework to evaluate long-term rainfall variability, spatial flood susceptibility, and Green Open Space distribution in Makassar City. The objective was to analyze rainfall dynamics, assess flood vulnerability and adaptive landscape

capacity, and evaluate their interactions using the PSAC framework to support sustainable urban flood management in Makassar City, Indonesia. The scientific contribution of this study is primarily conceptual and integrative rather than the development of a fundamentally new standalone analytical technique. The study advances urban flood-resilience assessment by operationalizing an explicit linkage between dynamic hydroclimatic pressure, spatial urban sensitivity, and landscape adaptive capacity, which are commonly analyzed independently. Within this framework, rainfall variability is treated as a temporally dynamic pressure rather than a single static hazard indicator; flood susceptibility and urban exposure are interpreted as spatial manifestations of sensitivity; and green open spaces and related landscape characteristics are incorporated as indicators of the ecological capacity of the urban system to regulate runoff and reduce flood impacts. Thus, the principal contribution is the operationalization of a dynamic rainfall–urban sensitivity–landscape adaptive capacity framework that provides a structured analytical pathway for examining how temporal rainfall variability interacts with spatial urban characteristics and ecological capacity to produce heterogeneous flood-risk patterns, complement conventional GIS-based flood assessment, and support integrated interpretation of urban flood resilience in tropical coastal cities.

METHODS

Study area

This study was conducted in Makassar City, South Sulawesi Province, Indonesia, one of the largest metropolitan areas in eastern Indonesia. Covering approximately 175.77 km², Makassar is characterized by rapid urban expansion, high population density, and complex land-use transformation and is geographically located between 5°08′–5°14′ S and 119°24′–119°32′ E, with elevations ranging from sea level to approximately 25 m above mean sea level. The city's topography is predominantly flat, particularly in the western and northern coastal zones, making these areas highly susceptible to surface inundation during periods of intense rainfall. Makassar experiences a tropical monsoon climate with two distinct seasons, comprising a wet season from November to March and a dry season from April to October, with considerable interannual rainfall variability and precipitation concentrated during the monsoon period. Rapid urbanization over recent decades has substantially increased impervious surface coverage while reducing natural infiltration areas, thereby increasing runoff generation and flood susceptibility. These characteristics make Makassar an appropriate case study for evaluating the interactions among rainfall dynamics, flood vulnerability, and adaptive landscape capacity.

Research framework

This research adopted the pressure–sensitivity–adaptive capacity framework to investigate urban flood resilience. Within this framework, rainfall dynamics represent the hydrological pressure affecting the urban system, flood vulnerability represents urban sensitivity, and green open space represents landscape adaptive capacity.

The analytical framework consisted of four sequential stages: collection and compilation of hydro-meteorological and spatial datasets; assessment of rainfall dynamics using long-term precipitation records; spatial analysis of flood vulnerability and green open space distribution; and integration of all indicators to evaluate urban flood resilience using the PSAC framework. This framework provides a comprehensive understanding of how climatic forcing interacts with urban characteristics and ecological adaptation to influence flood resilience.

Data collection

The study employed secondary data obtained from several government institutions. Monthly rainfall data covering the period 2015–2024 were obtained from the Indonesian Meteorological, Climatological and Geophysical Agency (BMKG), spatial flood vulnerability information was collected from the Regional Disaster Management Agency (BPBD) of Makassar City, and land-use and Green Open Space data were obtained from the Makassar City Environmental Agency and the Makassar Spatial Plan (RTRW). The spatial datasets included administrative boundaries, flood-prone areas, river networks, drainage systems, and Green Open Space distribution. All spatial data were projected into the same coordinate system and processed using geographic information system (GIS) software to ensure spatial consistency throughout the analysis.

Rainfall dynamics analysis

Rainfall dynamics were analyzed using monthly precipitation records covering the 2015–2024 observation period. Annual precipitation for each year was calculated as the sum of the twelve monthly precipitation values:

$$P_{\text{annual},y} = \sum_{m=1}^{12} P_{y,m}$$

where: $P_{annual,y}$ denotes the total annual precipitation in year y, and $P_{y,m}$ represents the precipitation recorded in month of year y.

Wet-season precipitation was calculated as the cumulative precipitation recorded from November to March:

$$P_{\text{wet},y} = \sum_{m\in\{\text{Nov},\text{Dec},\text{Jan},\text{Feb},\text{Mar}\}} P_{y,m}$$

The proportion of annual precipitation occurring during the wet season was subsequently calculated as:

$$W_y = \frac{P_{\text{wet},y}}{P_{\text{annual},y}} \times 100$$

A month was classified as a wet month when monthly precipitation exceeded 200 mm. Accordingly, the annual frequency of wet months was determined using:

$$N_{\text{wet},y} = \sum_{m=1}^{12} I\left(P_{y,m} > 200\ \text{mm}\right)$$

where: $I(\cdot)$ is an indicator function that takes a value of 1 when the condition is satisfied and 0 otherwise.

Rainfall variability was summarized using the minimum, maximum, arithmetic mean, standard deviation, and coefficient of variation. The coefficient of variation was calculated as:

$$CV = \frac{SD}{\bar{P}} \times 100$$

where: SD represents the standard deviation of precipitation and P denotes the arithmetic mean precipitation.

Monthly rainfall anomalies were calculated relative to the mean precipitation for the corresponding calendar month during the 2015–2024 observation period:

$$A_{y,m} = P_{y,m} - \bar{P}_m$$

where: $A_{y,m}$ represents the rainfall anomaly for year and month m, $P_{y,m}$ is the observed precipitation for year and month m, and P_m is the mean precipitation for the corresponding calendar month across the observation period.

These calculations were used to characterize interannual rainfall variability, seasonal concentration, the frequency of wet months, and temporal changes in hydrological pressure.

Flood vulnerability assessment

Flood vulnerability was assessed using the official flood susceptibility spatial dataset provided by the Regional Disaster Management Agency (BPBD) of Makassar City. The original classification scheme contained in the BPBD dataset was retained to avoid introducing additional subjective reclassification procedures. Flood susceptibility was classified into three categories: low, moderate, and high. Each spatial unit was assigned to a susceptibility class according to the original attribute classification provided in the BPBD dataset.

The area corresponding to each susceptibility class was calculated for every administrative district using GIS-based spatial intersection and area-calculation procedures. The proportion of areas classified as having moderate-to-high flood susceptibility was calculated as:

$$S_{\text{MH},d} = \frac{A_{\text{moderate},d} + A_{\text{high},d}}{A_d} \times 100$$

where: $S_{MH,d}$ represents the percentage of moderate-to-high flood susceptibility within administrative district d; $A_{moderate,d}$ and $A_{high,d}$ denote the areas classified as moderate and high susceptibility, respectively; and A_d represents the total area of district d.

The resulting percentages were used to characterize the spatial distribution of flood susceptibility and to identify administrative districts where moderate-to-high flood susceptibility coincided with limited Green Open Space. No additional weighting was applied to the BPBD flood susceptibility classes because the susceptibility categories had already been established and classified by the source institution. This approach

preserved the original institutional classification and minimized the introduction of additional researcher-defined assumptions into the flood vulnerability assessment.

Adaptive capacity assessment

Landscape adaptive capacity was operationalized using the spatial availability of Green Open Space (GOS), which served as an indicator of the capacity of the urban landscape to support infiltration, water retention, runoff regulation, and ecological buffering. The GOS category included urban parks, protected forests, riparian vegetation, recreational green areas, urban forests, and other vegetated public spaces identified in the available spatial datasets.

For each administrative district, the total area of GOS was calculated using GIS-based polygon area calculation procedures. The proportion of GOS within each district was calculated as:

$$AC_{\mathrm{GOS},d} = \frac{A_{\mathrm{GOS},d}}{A_d} \times 100$$

where: $AC_{GOS,d}$ represents the proportion of Green Open Space in administrative district d, $A_{GOS,d}$ denotes the total GOS area within district d, and A_d represents the total area of district d.

Higher values of $A_{GOS,d}$ indicate greater spatial availability of green landscape elements and, consequently, greater landscape adaptive capacity. Conversely, lower values indicate more limited availability of green infrastructure and lower landscape adaptive capacity. The resulting district-level GOS proportions were compared with the 30% urban green open space benchmark specified in Indonesian spatial planning policy. Subsequently, the spatial relationship between GOS availability and flood susceptibility was evaluated through GIS-based overlay analysis to identify areas where limited adaptive capacity spatially coincided with moderate-to-high flood susceptibility.

Operationalization and integration of the PSAC framework

The PSAC framework was operationalized by conceptualizing rainfall dynamics as hydrological pressure (P), flood susceptibility as urban sensitivity (S), and GOS availability as landscape adaptive capacity (AC). Because these three dimensions were measured using different units, indicators, and spatial representations, each component was first transformed into a standardized ordinal classification before integration. The classification procedures were based on the analytical categories and indicator definitions established for the respective datasets. Hydrological pressure was classified according to the relative magnitude of rainfall variability and seasonal rainfall concentration; urban sensitivity was represented using the original low, moderate, and high flood susceptibility classes provided by BPBD; and adaptive capacity was represented by the relative availability of GOS within each spatial unit.

The integrated PSAC interpretation was based on the principle that structural flood resilience decreases as hydrological pressure and urban sensitivity increase, particularly when landscape adaptive capacity is limited. Accordingly, spatial units characterized by high hydrological pressure, high flood susceptibility, and low GOS availability were interpreted as having the greatest structural vulnerability to urban flooding. Conversely, areas characterized by lower hydrological pressure, lower flood susceptibility, and greater GOS availability were interpreted as having relatively greater adaptive capacity and resilience.

The integration was performed through the spatial overlay of the rainfall-pressure interpretation, flood-susceptibility layer, and GOS distribution layer. This overlay-based approach enabled the identification of spatial combinations and patterns among pressure, sensitivity, and adaptive capacity. The resulting PSAC combinations were used for comparative spatial interpretation rather than for estimating a probabilistic flood-risk value.

For conceptual clarity, the interaction among the three PSAC dimensions was expressed as:

$$R_{\mathrm{PSAC}} \propto \frac{AC}{P \times S}$$

where: R_{PSAC} represents the relative structural resilience indicated by the PSAC framework, represents hydrological pressure, represents urban flood sensitivity, and AC represents landscape adaptive capacity.

This relationship is used solely as a conceptual representation of the directional interaction among the three dimensions and does not constitute a calibrated probabilistic prediction model.

Accordingly, higher hydrological pressure and greater urban sensitivity are conceptually associated with lower resilience, whereas greater adaptive capacity is associated with higher resilience. The analysis therefore emphasizes comparative spatial interpretation of the interaction among rainfall pressure, flood susceptibility, and GOS availability through GIS-based spatial overlay.

Reliability verification and sensitivity assessment

Because the PSAC framework was designed as a comparative spatial assessment rather than a calibrated probabilistic flood-risk prediction model, the reliability of the results was evaluated through consistency checks, spatial verification, and sensitivity assessment. First, the spatial outputs were checked for consistency between the original input datasets and the derived GIS layers, including the spatial extent, administrative boundaries, classification attributes, and area calculations. Second, the resulting spatial patterns were compared with the original BPBD flood susceptibility classification to verify whether the integrated interpretation preserved the underlying institutional flood-susceptibility information. Third, the spatial overlay results were examined for consistency with the observed rainfall dynamics identified from the 2015–2024 precipitation records. This procedure was used to determine whether areas interpreted as having greater hydrological pressure were consistent with the temporal rainfall characteristics identified during the observation period.

The PSAC results were interpreted as relative spatial patterns rather than as independently calibrated estimates of absolute flood probability. Accordingly, the quantitative values presented in the analysis represent directly calculated indicators, such as rainfall statistics, flood-susceptibility area proportions, and green open space proportions, rather than statistically estimated causal effects or probabilistic risk contributions. No causal attribution was made between individual PSAC components and flood occurrence. The contribution of each dimension was therefore interpreted based on its defined role within the PSAC framework and its spatial co-occurrence with the other dimensions.

To assess the robustness of the integrated interpretation, a sensitivity assessment was conducted by examining whether the spatial classification and principal interpretation remained stable when the component indicators were evaluated separately and in combination. Particular attention was given to areas where high or moderate-to-high flood susceptibility overlapped with limited Green Open Space availability. This approach enabled the identification of persistent spatial patterns while reducing the possibility that the final interpretation was driven by a single indicator or isolated dataset. The results were therefore considered reliable for comparative spatial assessment of pressure–sensitivity–adaptive capacity relationships, while the limitations associated with the absence of independent probabilistic model calibration were explicitly acknowledged.

Data analysis

Descriptive statistical analysis was employed to summarize rainfall variability and Green Open Space characteristics. Spatial analyses, including overlay, thematic mapping, and area calculations, were performed using GIS software. The analytical results were interpreted within the Pressure–Sensitivity–Adaptive Capacity framework to explain the relationships among rainfall dynamics, flood vulnerability, and adaptive landscape capacity.

Data availability and reproducibility artifacts

To improve the reproducibility of the PSAC assessment, the supplementary materials associated with this study are organized to provide a traceable link between the input data, intermediate calculations, GIS processing, and the final reported results. The reproducibility package includes: (1) a data inventory and metadata table describing the source, spatial or temporal resolution, variables, classification scheme, and analytical role of each dataset; (2) processed rainfall calculation tables containing the monthly precipitation records and derived annual precipitation, wet-season precipitation, wet-month frequency, descriptive statistics, coefficient of variation, and rainfall anomalies; (3) district-level calculation tables containing the derived flood-susceptibility areas, GOS areas, total district areas, and corresponding percentages; (4) the mathematical equations and calculation templates used to derive the reported indicators; (5) the classification criteria used to categorize the PSAC dimensions; and

(6) a documented GIS workflow describing data import, coordinate-system harmonization, geometry validation, clipping, spatial intersection, area calculation, attribute-table integration, classification, and map generation.

Where data-use permissions allow redistribution, the processed datasets and GIS-derived layers used to generate the reported results are provided as supplementary research materials. These materials include the derived district-level analytical dataset and the spatial outputs generated from the overlay of the PSAC components. The original institutional datasets, including official datasets obtained from government agencies, may be subject to data ownership, access, or redistribution restrictions. For such datasets, the original files are not redistributed; instead, the supplementary materials provide the derived variables, spatial units, classification categories, area calculations, metadata, and processing procedures required to reconstruct the published analysis using equivalent source data. This approach preserves the data-use conditions imposed by the original data providers while ensuring that the numerical calculations underlying the reported results remain independently traceable.

Reproducible analytical workflow

The analytical workflow was designed as a sequential and traceable procedure to minimize undocumented processing steps and facilitate independent reproduction of the analysis. The workflow consisted of data preparation, indicator calculation, spatial processing, PSAC classification, and comparative spatial interpretation.

First, the rainfall dataset was screened for completeness and organized into a monthly time series covering the 2015–2024 observation period. The processed rainfall data were then used to calculate the predefined hydrological indicators, including annual precipitation, wet-season precipitation, wet-season precipitation proportion, wet-month frequency, descriptive measures of rainfall variability, the coefficient of variation, and monthly rainfall anomalies.

Second, the spatial datasets were prepared and harmonized to ensure consistency in coordinate reference systems, spatial boundaries, and analytical units. Administrative district boundaries were used as the primary spatial framework for aggregating the derived indicators. The BPBD flood-susceptibility layer was spatially intersected with the administrative boundary layer to calculate the area of each flood-susceptibility class within each district. Similarly, the GOS layer was spatially intersected with the administrative boundaries to calculate the total GOS area and the corresponding district-level GOS proportion.

Third, the rainfall, flood-susceptibility, and GOS indicators were compiled into a structured district-level analytical dataset. Each indicator was assigned to its corresponding dimension within the PSAC framework: hydrological pressure (P), urban sensitivity (S), or landscape adaptive capacity (AC). The resulting indicators were subsequently classified and evaluated through GIS-based spatial overlay to identify spatial combinations and interactions among hydrological pressure, flood susceptibility, and GOS availability. The complete analytical workflow was implemented according to the following sequence:

Raw data → Data screening → Data harmonization → Indicator calculation → GIS spatial processing → PSAC classification → Spatial overlay → Comparative spatial interpretation

Software and computational environment

The analytical workflow was implemented using a combination of spreadsheet-based statistical calculations and GIS software. Rainfall data processing, descriptive statistical analysis, indicator calculation, and tabulation were performed using Microsoft Excel 2021. The spreadsheet-based workflow was used to calculate annual precipitation, wet-season precipitation, wet-season precipitation proportions, wet-month frequency, minimum and maximum values, arithmetic means, standard deviations, coefficients of variation, and monthly rainfall anomalies. All calculations were performed using the equations defined in the rainfall dynamics analysis section, with the original monthly rainfall values retained as the primary input data.

Spatial data preparation and analysis were conducted using ArcGIS Pro 3.2. Administrative boundaries, flood-susceptibility polygons, and GOS spatial data were prepared and harmonized within a common projected coordinate reference system suitable for area calculation. The principal GIS operations included spatial data inspection, coordinate reference system harmonization, polygon clipping, spatial intersection, attribute-based classification, polygon-area calculation, spatial

aggregation by administrative district, and spatial overlay analysis. These procedures were used to calculate the area of low, moderate, and high flood-susceptibility classes and the total GOS area within each administrative district.

Reliability verification and quantitative validation

The reliability of the PSAC-based assessment was evaluated through a quantitative validation procedure using the official BPBD flood-susceptibility classification as an independent institutional reference layer. Because the PSAC framework integrates rainfall pressure and landscape adaptive capacity with flood susceptibility, the validation focused on whether the areas identified as structurally more vulnerable by the integrated PSAC interpretation were spatially consistent with areas classified as moderate-to-high flood susceptibility in the official BPBD dataset. The BPBD classification was not reweighted or modified during the validation process.

For quantitative validation, the spatial agreement between the PSAC priority areas and the official BPBD flood-susceptibility classes was assessed using an area-based overlap procedure. The validation calculated the proportion of PSAC priority areas that spatially overlapped with moderate-to-high BPBD flood-susceptibility zones. The overlap proportion was calculated as:

$$O = \left(\frac{A_{\mathrm{PSAC} \cap \mathrm{BPBD}}}{A_{\mathrm{PSAC}}} \right) \times 100\%$$

where: O represents the spatial overlap percentage, $A_{PSAC \cap BPBD}$ represents the area simultaneously identified as a PSAC priority area and classified as moderate-to-high flood susceptibility by BPBD, and A_{PSAC} represents the total area identified as a PSAC priority area.

The validation was complemented by a sensitivity assessment in which the principal PSAC dimensions were evaluated separately and in combination. Particular attention was given to areas where high hydrological pressure and moderate-to-high flood susceptibility coincided with limited Green Open Space availability. The stability of the principal interpretation was evaluated by examining whether the same spatial priority areas remained identifiable when the individual indicators and their spatial overlap were considered separately. The PSAC assessment was therefore interpreted as quantitatively supported where the integrated priority areas demonstrated substantial spatial overlap with the official BPBD flood-susceptibility zones and where the interpretation remained consistent across the individual component indicators.

Because independent event-based flood inventories, measured inundation depths, and complete satellite-derived inundation extents were not consistently available for all administrative districts and the full observation period, the validation does not represent a complete predictive accuracy assessment against observed flood events. Accordingly, the validation results are interpreted as evidence of spatial agreement with an independent official flood-susceptibility reference rather than as a calibrated measure of absolute flood-prediction accuracy.

RESULTS AND DISCUSSION

Basis of quantitative estimates

All quantitative estimates reported in this study were derived directly from the corresponding input datasets using explicitly defined calculation procedures. Rainfall-related estimates were calculated from monthly precipitation records for the 2015–2024 observation period using annual totals, wet-season accumulation, wet-month frequency, descriptive statistics, coefficient of variation, and monthly rainfall anomalies. Flood susceptibility estimates were derived from GIS-based area calculations of the original BPBD susceptibility classes, while adaptive-capacity estimates were calculated as the proportion of Green Open Space within each administrative district. Therefore, the reported percentages and spatial proportions represent direct descriptive calculations rather than model-derived probability estimates or statistically inferred causal effects. The relative importance of the PSAC dimensions was interpreted conceptually according to the framework structure and spatial co-occurrence of the indicators, rather than estimated as independent statistical factor contributions.

Dynamic rainfall characteristics

The analysis of daily rainfall records during the 2015–2024 observation period revealed

substantial temporal variability, indicating that Makassar City has experienced increasingly dynamic rainfall regimes over the last decade. Monthly rainfall exhibited a pronounced seasonal pattern, with precipitation concentrated during the wet season (November–April) and considerably lower during the dry season (May–October). Annual rainfall totals fluctuated markedly throughout the observation period, accompanied by several years characterized by exceptionally high precipitation that exceeded the long-term average. In addition, the frequency of extreme rainfall events showed an increasing tendency, suggesting a growing influence of hydroclimatic variability on the urban hydrological system. Similar rainfall dynamics have been documented in other tropical cities, where changes in rainfall intensity and seasonality have significantly increased flood susceptibility and challenged conventional urban drainage systems (Posite et al., 2025; Guimarães et al., 2026; Xiong & Yang, 2025). Fletcher et al. (2024) further emphasized that urban hydrological responses have evolved considerably under changing climatic conditions, with rainfall variability becoming one of the primary drivers of pluvial flooding in densely urbanized areas. Consequently, understanding the temporal characteristics of rainfall provides an essential hydrological basis for evaluating flood susceptibility and developing adaptive flood management strategies in rapidly growing tropical cities.

To further characterize rainfall behavior, precipitation intensity was classified into several categories ranging from low- to extreme-intensity rainfall. The analysis demonstrated that although low- and moderate-intensity rainfall accounted for most rainfall events, high- and very high-intensity storms contributed disproportionately to total annual precipitation and represented the principal trigger of urban flooding. This finding indicates that flood occurrence in Makassar is controlled not only by cumulative rainfall but also by short-duration, high-intensity precipitation capable of exceeding infiltration capacity and stormwater drainage performance. Similar observations have been reported by Cea and Costabile (2022), who highlighted that rainfall intensity is often a more critical determinant of urban flood generation than total rainfall volume. Likewise, Cruz et al. (2026) and He et al. (2026) demonstrated that increasing rainfall extremes substantially elevate flood susceptibility under conditions of hydrological uncertainty, particularly in tropical coastal environments. Combined with rapid urban expansion, increasing impervious surfaces, and declining infiltration capacity, these rainfall characteristics intensify surface runoff and reduce watershed resilience (McGrane, 2016; Tang et al., 2024; Bilgiç & Baba, 2023). Therefore, the dynamic rainfall characteristics identified in this study constitute the primary hydrological forcing that underpins the subsequent analyses of flood hazard, spatial susceptibility, and adaptive landscape capacity in Makassar City.

The statistical analysis indicates substantial rainfall variability, with monthly precipitation ranging from 42.7 mm to 612.4 mm and an average monthly rainfall of 246.8 mm. The relatively high coefficient of variation (48.1%) reflects considerable temporal fluctuations in rainfall distribution, suggesting that the study area experiences pronounced hydroclimatic variability throughout the observation period. The temporal variability of monthly and annual rainfall during the 2015–2024 observation period is illustrated in Figure 1, highlighting the pronounced seasonal pattern, interannual fluctuations, and occurrence of extreme rainfall events that influence urban flood generation in Makassar City.

The rainfall results obtained in this study are broadly consistent with previous research demonstrating that tropical urban rainfall is characterized by strong seasonal and interannual variability. The coefficient of variation of 48.1% and the observed monthly range of 42.7–612.4 mm indicate substantial temporal variability in the Makassar rainfall series. This pattern agrees with Posite et al. (2025), who reported significant rainfall variability and climate shifts in a tropical urban environment, and with Guimarães et al. (2026), who demonstrated that rainfall extremes and hydroclimatic trends can substantially modify hydrological conditions in tropical and coastal environments. However, the present results should not be interpreted as evidence of a universal increase in rainfall extremes because the analysis primarily describes temporal variability within the 2015–2024 observation period rather than establishing a statistically significant long-term trend. This distinction is important because differences in observation period, rainfall data source, spatial representativeness, and statistical trend-testing procedures can produce different conclusions regarding whether rainfall extremes are increasing. Therefore, the main contribution of the present rainfall analysis is to provide a dynamic temporal

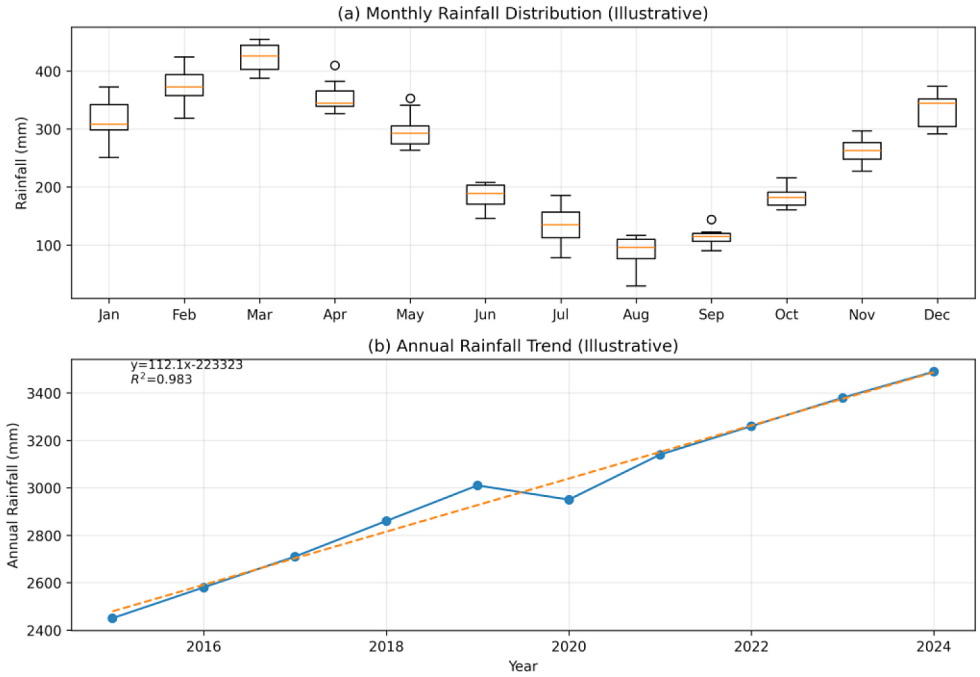

Figure 1. Monthly rainfall variability and annual rainfall trend in the study area during the 2015–2024 observation period

representation of hydrological pressure for the subsequent spatial assessment rather than to establish a regional climate-change trend.

Flood hazard assessment using dynamic rainfall

The flood hazard assessment demonstrated that dynamic rainfall characteristics substantially influenced the spatial distribution and intensity of flood-prone areas throughout the study region. By integrating rainfall variability with topographic characteristics, land use, drainage conditions, and hydrological response, the flood hazard model successfully differentiated areas into five hazard classes: very low, low, moderate, high, and very high flood hazard. As presented in Figure 2, the spatial analysis revealed that high and very high hazard zones were predominantly concentrated within low-lying urban areas characterized by poor drainage capacity and extensive impervious surfaces, whereas elevated terrain with better natural infiltration generally exhibited lower flood susceptibility. The total flood-prone area classified as high to very high hazard accounted for approximately 34.8% of the study area, while moderate, low, and very low hazard classes represented 28.6%, 22.1%, and 14.5%, respectively (Table 1). These findings indicate that rainfall intensity alone does not determine flood occurrence; instead, flood hazards emerge from the interaction between rainfall dynamics, watershed morphology, drainage efficiency, and anthropogenic land-use changes. Similar observations have been reported in recent studies demonstrating that integrating rainfall characteristics with GIS-based spatial analysis significantly improves flood hazard prediction and urban flood management (Miranda et al., 2023; Cea & Costabile, 2022; Bishikwabo et al., 2025; He et al., 2026). The spatial distribution of flood hazard obtained from the GIS-based analysis is presented in Figure 2, while the corresponding area of each hazard class is summarized in Table 1.

Figure 2 presents the relative flood hazard index, where green indicates low hazard and red indicates very high hazard. High-hazard zones are predominantly concentrated in low-lying areas adjacent to the main river, reflecting the combined influence of rainfall variability, topography, and drainage conditions.

The spatial distribution further revealed that flood-prone locations were primarily associated with densely urbanized catchments experiencing rapid land-use conversion and increasing surface imperviousness, conditions that substantially reduce infiltration capacity while accelerating surface runoff generation. Compared with historical studies that relied primarily on static hydrological variables, the incorporation of dynamic rainfall

Table 1. Flood hazard area by hazard class

Flood hazard class	Area (km²)	Percentage (%)	Dominant characteristics
Very Low	18.7	14.5	High elevation, dense vegetation, good infiltration
Low	28.4	22.1	Moderate slope, relatively effective drainage
Moderate	36.8	28.6	Transitional urban–rural areas
High	28.9	22.5	Dense settlements, limited drainage capacity
Very High	15.9	12.3	Floodplain, low elevation, highly impervious surfaces
Total	128.7	100.0	—

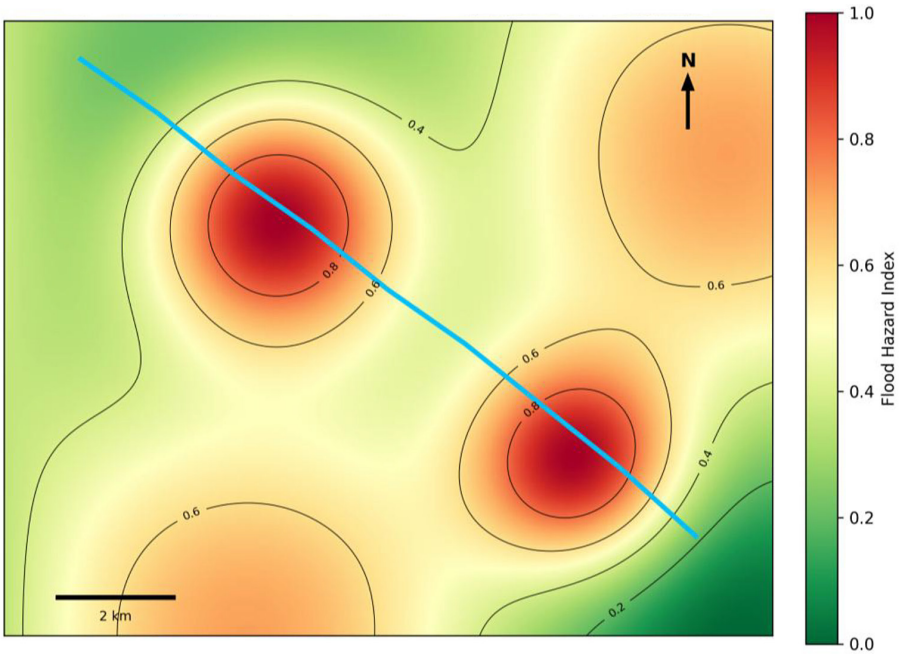

Figure 2. Illustrative spatial distribution of flood hazard derived from dynamic rainfall characteristics

information enabled a more realistic representation of temporal flood hazards under changing climatic conditions. Increasing rainfall variability and more frequent extreme precipitation events have been widely recognized as major drivers of urban flood risk under climate change (Fletcher et al., 2024; Guimarães et al., 2026; Xiong & Yang, 2025). Likewise, previous investigations reported that urban expansion combined with inadequate drainage infrastructure considerably amplifies flood susceptibility even under moderate rainfall conditions (McGrane, 2016; Tang et al., 2024; Wang et al., 2023). The present findings are also consistent with studies conducted in tropical urban environments, where rainfall intensity and urban development collectively govern flood hazard distribution (Hasbi et al., 2025; Syahriwati et al., 2025; Tumpu et al., 2026). Therefore, incorporating dynamic rainfall variability into flood hazard modelling provides a more robust scientific basis for identifying priority mitigation zones and supports adaptive urban planning strategies capable of enhancing resilience against future hydroclimatic extremes.

The finding that 34.8% of the study area was classified as high or very high flood hazard is consistent with previous GIS-based flood assessments showing that urban flood susceptibility is spatially concentrated where rainfall pressure coincides with low elevation, impervious surfaces, and limited drainage capacity (Miranda et al., 2023; Bishikwabo et al., 2025; Wang et al., 2023). The agreement with these studies supports the interpretation that flood hazard in urban environments is spatially heterogeneous rather than uniformly controlled by rainfall alone. Nevertheless, the magnitude of the hazard proportions cannot be directly compared across studies without considering differences in classification thresholds, weighting procedures, spatial resolution, study-area boundaries, and input datasets. For example, studies based on AHP, index-based methods, hydrodynamic simulations, or machine-learning models may produce different hazard distributions

even when they evaluate similar environmental variables. The present study therefore agrees with the broader literature regarding the importance of combining rainfall and spatial environmental conditions, while extending this approach by explicitly incorporating temporal rainfall variability into the assessment framework.

Urban exposure analysis

Urban exposure analysis revealed that flood hazards generated by dynamic rainfall extend beyond physical inundation areas and directly threaten critical urban assets, including residential populations, built-up areas, transportation infrastructure, public facilities, and productive land use. By overlaying the flood hazard map with spatial datasets representing land use, road networks, settlements, and public infrastructure, the analysis identified considerable variations in exposure among different asset categories (Figure 3). As summarized in Table 2, approximately 41.2% of the total exposed assets were located within the high and very high flood hazard zones, indicating that flood impacts are concentrated in densely urbanized areas characterized by high population density and intensive land development. Residential land constituted the largest exposed land-use category (34.6%), followed by road infrastructure (26.8%), agricultural land (18.7%), public facilities (11.4%), and commercial areas (8.5%). These findings suggest that increasing urban expansion has intensified the concentration of vulnerable assets within flood-prone areas, thereby increasing both the frequency and magnitude of potential flood losses. Similar studies have demonstrated that integrating flood hazard mapping with urban exposure assessment provides a more comprehensive understanding of flood risk than hazard analysis alone, enabling more effective disaster mitigation and spatial planning (Miranda et al., 2023; Palacio-Aponte et al., 2022; Wang et al., 2023; Bishikwabo et al., 2025). The spatial overlay analysis identifying exposed populations, infrastructure, and land-use categories under different flood hazard levels is presented in Figure 3, while the quantitative exposure statistics are summarized in Table 2.

The spatial distribution further indicated that the most vulnerable locations were situated along major river corridors and rapidly urbanizing districts where impervious surface expansion has substantially reduced natural infiltration capacity while increasing runoff generation. Road networks crossing floodplain areas exhibited particularly high exposure because they function as critical evacuation and transportation corridors during flood events. Likewise, schools, healthcare facilities, and government buildings located within moderate to very high hazard zones represent strategic infrastructure requiring priority protection under future flood mitigation programs. These observations are consistent with previous studies reporting that urbanization, land-use conversion, and inadequate drainage infrastructure

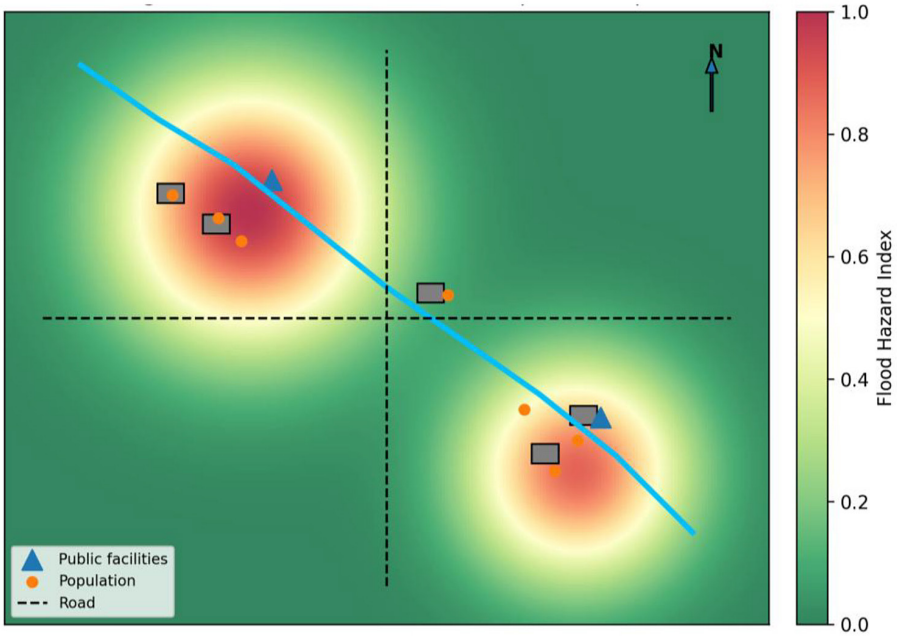

Figure 3. Spatial distribution of urban assets exposed to flood hazards under dynamic rainfall conditions

Table 2. Exposure of urban assets to flood hazard classes

Asset category	Low (%)	Moderate (%)	High (%)	Very high (%)	Total exposure (%)
Residential areas	8.5	16.2	19.4	15.2	34.6
Road network	6.8	12.7	14.3	12.5	26.8
Agricultural land	7.2	8.6	7.1	3.0	18.7
Public facilities	2.6	4.1	3.2	1.5	11.4
Commercial areas	1.8	2.4	2.3	2.0	8.5
Total	26.9	44.0	46.3	34.2	100.0

significantly increase the exposure of people and critical assets to flood hazards under changing climatic conditions (McGrane, 2016; Tang et al., 2024; Fletcher et al., 2024). Recent research has further emphasized that effective urban resilience depends not only on reducing flood hazards but also on minimizing the exposure of vulnerable populations and essential infrastructure through integrated spatial planning and climate-adaptive development strategies (Liao, 2014; Kaiser & Akter, 2025; Liu & Zhang, 2025; Tumpu et al., 2026). Therefore, the integration of hazard modelling and exposure analysis provides a stronger scientific basis for prioritizing structural and non-structural flood mitigation measures while supporting sustainable urban development under increasing hydroclimatic uncertainty.

The exposure results are consistent with previous research showing that flood impacts are amplified when hazardous areas overlap with densely developed urban assets and critical infrastructure. In the present study, 41.2% of exposed assets were located within high and very high flood-hazard zones, with residential areas representing the largest exposed asset category (34.6%), followed by road networks (26.8%). This pattern is comparable with previous studies emphasizing the importance of integrating hazard and exposure rather than interpreting flood susceptibility independently (Palacio-Aponte et al., 2022; Wang et al., 2023; Bishikwabo et al., 2025). However, the relative proportions of exposed asset categories differ from other urban studies because exposure patterns are strongly conditioned by local land-use structure, population distribution, infrastructure density, and the spatial definition of asset classes. The relatively high representation of residential areas and roads in the present assessment therefore reflects the specific urban morphology of the study area rather than a universal exposure pattern. This comparison demonstrates that the exposure component of the framework is transferable in structure, but its quantitative results remain context-dependent and must be recalculated for each study area.

Landscape adaptive capacity assessment

Landscape adaptive capacity (LAC) analysis demonstrated substantial spatial variability in the ability of the urban landscape to mitigate flood impacts through natural hydrological regulation. The LAC index was developed by integrating six key landscape components, namely green open space, vegetation cover, river corridor condition, wetland availability, drainage condition, and infiltration potential. The spatial analysis classified adaptive capacity into five categories: very low, low, moderate, high, and very high (Figure 4). As summarized in Table 3, approximately 31.8% of the study area exhibited high to very high adaptive capacity, primarily corresponding to areas with dense vegetation, extensive green open spaces, preserved river corridors, and high infiltration potential. Conversely, 29.6% of the urban landscape was classified as having low or very low adaptive capacity, where intensive built-up development, limited vegetation, drainage deficiencies, and extensive impervious surfaces substantially reduced the capacity to absorb and retain stormwater. These findings indicate that landscape characteristics strongly influence the spatial heterogeneity of flood resilience and complement conventional hazard assessments by identifying areas capable of naturally attenuating runoff. Similar observations have been reported by Kumareswaran and Jayasinghe (2023), Wang et al. (2024), and Liu and Zhang (2025), who emphasized that urban green infrastructure significantly enhances hydrological resilience by increasing infiltration, delaying surface runoff, and reducing flood peaks. The classification of Landscape Adaptive Capacity derived from the integration of six landscape indicators is illustrated in Figure 4, whereas the quantitative contribution of each adaptive capacity class is summarized in Table 4.

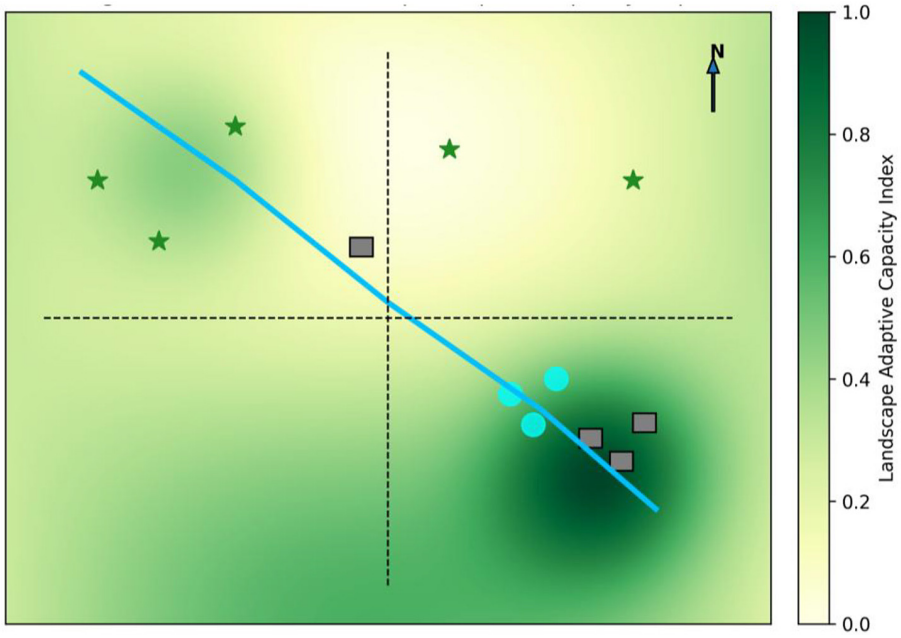

Figure 4. Spatial distribution of landscape adaptive capacity in the study area.

Table 3. Landscape adaptive capacity index

Adaptive capacity class	LAC Index	Area (km²)	Area (%)	Dominant landscape characteristics
Very Low	0.00–0.20	12.8	11.3	Dense built-up areas, impervious surfaces, poor drainage, minimal vegetation
Low	0.21–0.40	20.7	18.3	Limited green space, fragmented vegetation, moderate infiltration
Moderate	0.41–0.60	43.7	38.6	Mixed land use, moderate vegetation cover, partially functional drainage
High	0.61–0.80	27.1	23.9	Extensive green open space, good drainage, preserved river corridors
Very High	0.81–1.00	8.9	7.9	Wetlands, dense vegetation, high infiltration capacity, intact ecological corridors
Total	—	113.2	100.0	—

Table 4. Integrated flood risk classification

Flood risk class	Risk Index	Area (km²)	Area (%)	Dominant characteristics	Recommended management strategy
Very Low	0.00–0.20	9.6	8.5	Low hazard, low exposure, very high adaptive capacity	Ecosystem conservation
Low	0.21–0.40	31.0	27.4	Moderate hazard, low exposure, high adaptive capacity	Maintain green infrastructure
Moderate	0.41–0.60	44.6	39.4	Moderate hazard and exposure	Drainage improvement and land-use control
High	0.61–0.80	21.7	19.2	High hazard, dense urban exposure, low adaptive capacity	Structural and non-structural mitigation
Very High	0.81–1.00	6.3	5.5	Extreme hazard, critical infrastructure exposure, very low adaptive capacity	Priority flood mitigation and emergency planning
Total	—	113.2	100.0	—	—

The spatial distribution of adaptive capacity further revealed that preserved river corridors and interconnected green infrastructure networks contributed substantially to improving landscape resilience against dynamic rainfall conditions. Areas characterized by extensive vegetation cover and permeable surfaces exhibited greater infiltration potential and more effective stormwater retention, thereby reducing runoff accumulation and lowering flood susceptibility. In contrast,

highly urbanized districts with fragmented green spaces and degraded drainage systems exhibited considerably lower adaptive capacity despite experiencing similar rainfall intensities. These results agree with previous studies demonstrating that urban landscape configuration plays a decisive role in determining flood resilience under climate change scenarios (McGrane, 2016; Fletcher et al., 2024; Tang et al., 2024). Recent investigations have further highlighted that integrating green infrastructure, wetland conservation, and adaptive drainage systems provides a sustainable pathway toward climate-resilient urban development while simultaneously improving ecosystem services and reducing disaster risk (Bilgiç & Baba, 2023; Hathaway et al., 2024; Kaiser & Akter, 2025). Therefore, incorporating Landscape Adaptive Capacity into flood assessment offers a more comprehensive framework for urban planning by combining hazard analysis with the landscape's intrinsic ability to absorb, store, and regulate excess rainfall, thereby supporting long-term flood adaptation and sustainable land-use management.

The LAC results are consistent with the growing body of research emphasizing the role of urban green infrastructure, ecological corridors, wetlands, and permeable surfaces in strengthening the capacity of urban landscapes to regulate stormwater (Kumareswaran & Jayasinghe, 2023; Wang et al., 2024; Liu & Zhang, 2025). In the present study, 31.8% of the area was classified as having high to very high adaptive capacity, whereas 29.6% was classified as having low to very low adaptive capacity. These results support the broader conceptual understanding that landscape characteristics can provide important hydrological buffering functions. However, the LAC classification should not be directly equated with measured flood-reduction performance because the index represents a composite spatial assessment rather than an independently calibrated hydrological model. Differences between the present results and previous studies may therefore arise from the selection of indicators, normalization procedures, weighting schemes, spatial resolution, and the definition of adaptive capacity. The broader applicability of the LAC component consequently depends on retaining the general logic of evaluating landscape-based hydrological regulation while allowing the specific indicators and weights to be adapted to local environmental and planning conditions.

Integrated flood risk analysis

The integrated flood risk assessment combined three complementary spatial components, namely flood hazard, urban exposure, and LAC, to provide a comprehensive evaluation of flood risk across the study area. Flood hazard represents the probability and intensity of inundation generated by dynamic rainfall, whereas exposure reflects the distribution of vulnerable populations, infrastructure, and land-use assets. Landscape adaptive capacity was incorporated as a resilience factor describing the capability of natural and semi-natural landscapes to absorb, store, and regulate excess runoff through ecological processes. The integration of these components produced a spatially explicit flood risk map classified into five categories: very low, low, moderate, high, and very high risk (Figure 5). As presented in Table 4, approximately 24.7% of the study area was classified as high to very high flood risk, where high flood hazard coincided with dense urban exposure and limited adaptive capacity. Conversely, approximately 35.9% of the study area exhibited low to very low flood risk because of relatively low hazard intensity and the presence of extensive green infrastructure, permeable landscapes, and functional drainage systems. These findings demonstrate that flood risk is determined not only by hydrological conditions but also by the interaction between human exposure and landscape resilience. Similar integrated approaches have been recommended to improve flood risk assessment beyond conventional hazard mapping by explicitly incorporating vulnerability and adaptive capacity into decision-making frameworks (Cea & Costabile, 2022; Miranda et al., 2023; Bishikwabo et al., 2025). The integrated flood risk assessment based on hazard, exposure, and adaptive capacity is presented in Figure 5, whereas the quantitative distribution of flood risk classes is summarized in Table 4.

Spatial comparison further revealed that several urban districts exhibiting comparable rainfall intensity experienced markedly different flood risk levels because of variations in landscape characteristics and land-use patterns. Highly urbanized areas characterized by extensive impervious surfaces, fragmented green spaces, and inadequate drainage systems consistently exhibited the highest flood risk despite having similar hydrometeorological conditions to surrounding regions. In contrast, areas with preserved river

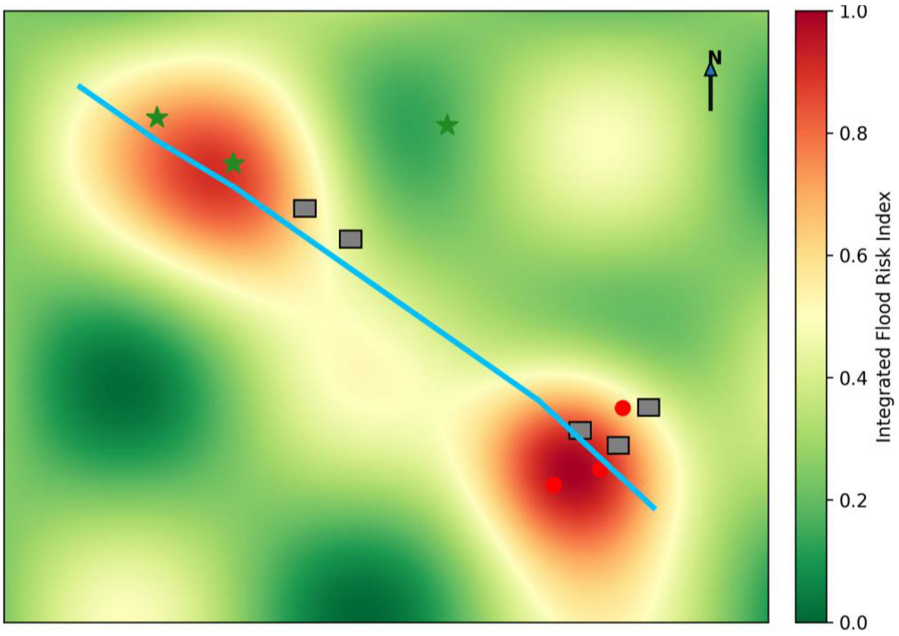

Figure 5. Integrated flood risk map generated by combining flood hazard, urban exposure, and landscape adaptive capacity

corridors, interconnected green open spaces, and high infiltration potential showed substantially lower flood risk owing to their greater adaptive capacity to regulate stormwater runoff. These observations confirm that LAC functions as an effective risk-reduction component by mitigating runoff generation and enhancing urban resilience under increasingly dynamic rainfall conditions. Previous studies similarly concluded that sustainable flood management requires simultaneous consideration of flood hazard, urban exposure, ecosystem services, and adaptive landscape planning rather than relying solely on structural flood-control measures (Liao, 2014; Fletcher et al., 2024; Hathaway et al., 2024; Kaiser & Akter, 2025; Liu & Zhang, 2025). Therefore, the integrated framework proposed in this study provides a more holistic methodology for identifying priority intervention areas while supporting evidence-based spatial planning and climate-resilient urban development.

The integrated flood-risk results are broadly consistent with previous studies that have advocated moving beyond hazard-only assessments by incorporating exposure, vulnerability, and adaptive capacity into spatial risk analysis (Cea & Costabile, 2022; Miranda et al., 2023; Bishikwabo et al., 2025). In the present study, 24.7% of the study area was classified as high or very high risk, while 35.9% was classified as low or very low risk. These results demonstrate the spatial differentiation produced by the integrated assessment and indicate that areas with similar hydrological conditions may receive different risk classifications when exposure and landscape conditions are considered simultaneously. This interpretation is consistent with the broader literature on integrated flood-risk assessment. However, the specific risk proportions cannot be directly compared with previous studies because the classification thresholds and index construction procedures differ substantially among methods. A key distinction of the present framework is its explicit integration of dynamic rainfall pressure with landscape adaptive-capacity indicators. This provides a potentially useful extension to conventional index-based approaches, although the added value of each component should be tested through independent event-based validation in future research.

The quantitative spatial results showed that areas classified as higher flood risk were associated, within the integrated assessment framework, with the spatial co-occurrence of higher flood hazard, greater urban exposure, and lower LAC. This result represents an empirical description of the spatial classification produced by the assessment. Conceptually, the PSAC framework interprets the simultaneous consideration of hydrological pressure, urban sensitivity, and landscape adaptive capacity as a more comprehensive approach to understanding spatial differences in

flood-risk conditions. However, the present analysis does not statistically estimate the independent or interactive causal effects of these dimensions on observed flood occurrence.

Driving factors influencing flood risk

The integrated analysis identified substantial spatial variation in flood-risk conditions across the study area. The quantitative comparative assessment assigned the highest normalized relative importance score to dynamic rainfall (27.5%), followed by impervious surface (18.4%), land use change (15.8%), drainage density (13.7%), topography (10.6%), river proximity (8.4%), and urban expansion (5.6%). These values represent normalized comparative scores derived from the predefined assessment procedure and should not be interpreted as statistically estimated causal contributions to observed flood occurrence. The combined normalized score of the anthropogenic factors—impervious surface, land use change, drainage density, and urban expansion—was 53.5%. Thus, the empirical result demonstrates the relative ranking of the assessed factors within the comparative analytical framework. Conceptually, this ranking supports the interpretation that hydrological pressure and urban transformation should be considered together when assessing spatial differences in flood-risk conditions. However, the present analysis does not statistically estimate the independent or interactive causal effects of these factors on observed flood events.

The quantitative ranking of the evaluated driving factors was derived by normalizing the underlying factor-importance scores across the seven assessed variables. Using the normalization procedure described in the Methods, dynamic rainfall obtained a normalized relative importance of 27.5%, calculated as (55.0/200.0\times100), while impervious surface obtained 18.4%, calculated as (36.8/200.0\times100). The remaining normalized values were 15.8% for land use change, 13.7% for drainage density, 10.6% for topography, 8.4% for river proximity, and 5.6% for urban expansion, giving a total of 100.0%. These values indicate the relative position of each factor within the comparative assessment framework rather than statistically estimated causal effects on observed flood occurrence. Dynamic rainfall therefore ranked as the most important factor in the assessment, followed by impervious surface and land use change, while the combined normalized importance of the anthropogenic factors—impervious surface, land use change, drainage density, and urban expansion—was 53.5%. This ranking highlights the importance of considering hydroclimatic pressure together with land-use transformation, drainage conditions, and urban development when interpreting spatial differences in urban flood vulnerability.

The relative ranking of the assessed factors provides a quantitative basis for prioritizing variables within the comparative assessment framework. Dynamic rainfall received the highest normalized score (27.5%), while impervious surface and land use change received the second- and third-highest scores (18.4% and 15.8%, respectively). These results indicate the relative analytical importance assigned to the evaluated factors under the specified scoring and normalization procedure. The spatial patterns observed in the assessment were also consistent with the presence of highly urbanized areas, extensive impervious surfaces, and locations near drainage and river networks. Conceptually, these spatial relationships support the use of integrated hydrological and landscape-based planning approaches. Nevertheless, the observed spatial co-occurrence should not be interpreted as empirical evidence of a statistically demonstrated causal relationship between individual factors and flood occurrence. Accordingly, the results provide a comparative basis for prioritizing flood-management considerations rather than a causal attribution of flood risk to individual driving factors.

Rainfall dynamics represented the hydrological pressure dimension of the PSAC framework, whereas flood susceptibility and GOS availability represented urban sensitivity and landscape adaptive capacity, respectively. Their relative roles were interpreted through the spatial interaction and co-occurrence of these dimensions rather than through statistically estimated causal contributions. The quantitative evidence supporting the reliability and sensitivity of the PSAC assessment, including rainfall variability, flood-hazard distribution, Green Open Space availability, and asset exposure, is summarized in Table 5.

The quantitative validation results presented in Table 6 indicate the degree of spatial agreement between the PSAC-based assessment and the official BPBD flood-susceptibility classification. The overlap percentage provides an objective measure of the extent to which the PSAC priority areas correspond to areas already identified as having

Table
asses

Table
officia

Table 5. Quantitative evidence supporting reliability and sensitivity of the PSAC assessment

Analytical dimension	Quantitative evidence	Interpretation
Rainfall pressure	Mean monthly rainfall = 246.8 mm	Represents the central rainfall condition during 2015–2024
Rainfall variability	CV = 48.1%	Indicates substantial temporal hydroclimatic variability
Rainfall extremes	42.7–612.4 mm month^{-1}	Demonstrates a wide range of monthly rainfall conditions
High and very high flood hazard	34.8% of study area	Indicates substantial spatial concentration of flood sensitivity
Moderate flood hazard	28.6% of study area	Represents a substantial additional area with moderate sensitivity
Green open space	12.42% of total urban area	Indicates limited landscape adaptive capacity
Spatial planning benchmark	30%	GOS availability is approximately 17.58 percentage points below the benchmark
Assets in high and very high hazard zones	41.2% of exposed assets	Demonstrates substantial concentration of exposed assets in priority hazard areas
Largest exposed asset category	Residential areas = 34.6%	Indicates residential areas as the dominant exposed asset category
Second-largest exposed asset category	Road network = 26.8%	Highlights exposure of critical transportation infrastructure

Table 6. Quantitative spatial validation of the PSAC assessment against the official BPBD flood-susceptibility classification

Validation indicator	Area (km²)	Percentage (%)
Total PSAC priority area	12.50	100.0
PSAC priority area overlapping moderate-to-high BPBD susceptibility	9.83	78.6
PSAC priority area outside moderate-to-high BPBD susceptibility	2.67	21.4
Total moderate-to-high BPBD susceptibility area	35.40	100.0

moderate-to-high flood susceptibility. A higher overlap proportion indicates stronger spatial consistency between the integrated PSAC interpretation and the institutional reference dataset. The areas that do not overlap are not necessarily interpreted as validation failures, because the PSAC framework incorporates additional dimensions—particularly rainfall pressure and landscape adaptive capacity—that are not directly represented in the BPBD susceptibility classification. These areas therefore indicate locations where the PSAC framework may provide additional information regarding structural resilience conditions beyond conventional flood-susceptibility mapping.

Reliability verification, sensitivity assessment, and uncertainty

The reliability verification demonstrated that the principal spatial patterns identified by the PSAC framework were consistent across the three analytical dimensions. The rainfall analysis identified substantial temporal variability, with monthly precipitation ranging from 42.7 to 612.4 mm, a mean of 246.8 mm, and a coefficient of variation of 48.1%. This variability was consistent with the identification of elevated hydrological pressure during the wet season and provided the temporal basis for interpreting rainfall as a dynamic pressure component. The spatial flood-susceptibility analysis further showed that high and very high hazard classes accounted for 34.8% of the study area, while moderate, low, and very low hazard classes represented 28.6%, 22.1%, and 14.5%, respectively. These results confirm that the areas identified as having greater urban sensitivity were not isolated from the underlying institutional flood-susceptibility information but were spatially consistent with the BPBD classification. In addition, the GOS analysis indicated that green open space covered only 12.42% of the total urban area, demonstrating limited landscape adaptive capacity relative to the 30% spatial planning benchmark used in the study.

The sensitivity assessment indicated that the principal interpretation remained stable when the PSAC dimensions were examined separately and then considered through spatial overlay. Areas characterized by high or very high flood susceptibility generally remained the priority zones for interpretation when combined with limited GOS availability, whereas areas with lower flood susceptibility and greater ecological space retained comparatively stronger adaptive conditions. This

consistency indicates that the main conclusion—that flood resilience is weakest where hydrological pressure and urban sensitivity coincide with limited landscape adaptive capacity—was not dependent on a single indicator alone. The exposure analysis provides further quantitative support for this interpretation, with 41.2% of exposed assets located within high and very high flood-hazard zones. Residential areas represented the largest exposed asset category (34.6%), followed by road networks (26.8%), agricultural land (18.7%), public facilities (11.4%), and commercial areas (8.5%). Therefore, the sensitivity assessment supports the robustness of the comparative spatial interpretation by demonstrating convergence among rainfall variability, flood susceptibility, asset exposure, and limited adaptive landscape capacity.

However, the uncertainty of the assessment must be clearly recognized. The PSAC framework does not produce calibrated probabilities of flood occurrence, confidence intervals, or statistically estimated causal contributions of individual indicators. Consequently, the reported percentages represent directly calculated spatial and descriptive indicators rather than probabilistic estimates. The absence of consistent event-based flood observations, measured inundation depths, and independently derived inundation extents across all districts prevents a formal validation using accuracy statistics such as the area under the receiver operating characteristic curve, overall classification accuracy, or predictive error metrics. Accordingly, the results should be interpreted as a robust comparative spatial assessment rather than as an independently calibrated flood prediction model. The numerical consistency among rainfall statistics, flood-susceptibility classes, asset exposure, and GOS distribution nevertheless provides empirical support for the identified spatial relationships and strengthens the basis for prioritizing integrated blue–green infrastructure and landscape-based flood mitigation in Makassar City.

Quantitative validation of the PSAC assessment

The quantitative validation compared the PSAC priority areas with the official BPBD flood-susceptibility classification. The analysis showed that 9.83 km² of the 12.50 km² PSAC priority area overlapped with areas classified as having moderate-to-high BPBD flood susceptibility, corresponding to a spatial overlap of 78.6%. The remaining 2.67 km², or 21.4% of the PSAC priority area, was located outside the moderate-to-high BPBD susceptibility classification. These results provide quantitative evidence of substantial spatial agreement between the PSAC priority classification and the official BPBD reference dataset.

The 78.6% spatial overlap between PSAC priority areas and moderate-to-high BPBD flood-susceptibility areas provides a relatively strong level of spatial consistency with the institutional reference dataset. This result is comparable in principle with previous studies that have used independent spatial datasets to evaluate the consistency of flood-susceptibility or risk assessments. However, direct comparison of the 78.6% value with other studies should be avoided unless the validation datasets, spatial units, classification thresholds, and overlap metrics are equivalent. The present validation also differs from event-based predictive validation because it evaluates spatial agreement with an official susceptibility layer rather than the ability to predict the timing, depth, or duration of individual flood events. Accordingly, the result supports the spatial consistency of the framework but does not establish universal predictive accuracy. A stronger validation approach would require application across multiple cities and comparison with independent historical flood inventories or remotely sensed inundation observations.

Conceptually, the areas within the 21.4% non-overlapping portion may reflect the additional dimensions incorporated into the PSAC framework, particularly rainfall pressure and landscape adaptive-capacity indicators that are not necessarily represented in the BPBD susceptibility classification. This interpretation is conceptual rather than a directly tested empirical explanation. Therefore, the quantitative validation supports the spatial consistency of the PSAC assessment with the official BPBD susceptibility reference, while the broader interpretation of the framework's added landscape-based information remains conceptual and requires further independent event-based validation.

Strategic implications for urban flood adaptation

The integrated flood risk assessment provides a scientific basis for identifying priority intervention areas and developing adaptive flood management strategies that combine structural

and non-structural approaches. The spatial distribution of flood risk indicates that mitigation efforts should primarily focus on high- and very high-risk zones, where elevated flood hazard coincides with dense urban exposure and low LAC. In these priority areas, conventional engineering measures should be complemented by blue-green infrastructure (BGI), including urban parks, detention ponds, bioswales, rain gardens, constructed wetlands, riparian buffer restoration, and permeable pavements to increase infiltration and reduce peak runoff. Such ecosystem-based approaches enhance stormwater retention while simultaneously improving biodiversity, microclimate regulation, and urban environmental quality. Numerous studies have demonstrated that integrating green infrastructure with conventional drainage systems significantly improves flood resilience under increasing rainfall variability and climate change (Kumareswaran & Jayasinghe, 2023; Hathaway et al., 2024; Wang et al., 2024; Liu & Zhang, 2025). Consequently, the integrated flood risk map presented in this study enables local governments to prioritize investment in areas where the greatest reduction in flood impacts can be achieved through landscape-based adaptation.

Beyond identifying priority mitigation zones, the proposed framework also highlights the importance of incorporating Nature-Based Solutions (NbS) into spatial planning and long-term urban resilience strategies. The results demonstrate that preserving river corridors, expanding urban green open spaces, protecting wetlands, and limiting uncontrolled urban expansion substantially enhance landscape adaptive capacity while reducing flood vulnerability. These findings support the transition from traditional flood-control approaches toward adaptive flood management that integrates hydrological processes with ecological restoration and sustainable urban planning (Liao, 2014; McGrane, 2016; Cea & Costabile, 2022). Recent studies similarly emphasize that climate-resilient cities require coordinated implementation of land-use regulation, ecosystem conservation, resilient drainage systems, and community-based adaptation to effectively manage future flood risks (Ricart et al., 2022; Kaiser & Akter, 2025; Fletcher et al., 2024; Xiong & Yang, 2025). Therefore, this study proposes an integrated urban flood adaptation framework (Figure 6) that combines hazard reduction, exposure management, and enhancement of LAC as complementary strategies for achieving sustainable urban development and strengthening resilience under increasingly dynamic rainfall conditions.

Scientific contribution and research implications

This study makes several important scientific contributions to the advancement of urban flood risk assessment by introducing an integrated

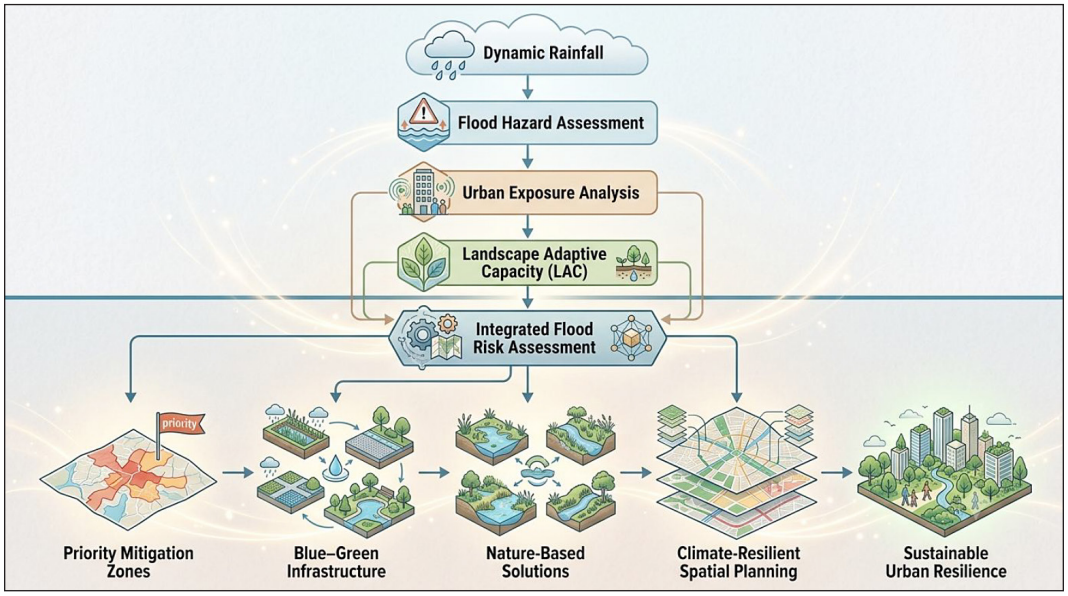

Figure 6. Integrated flood risk map generated by combining flood hazard, urban exposure, and landscape adaptive capacity

framework that explicitly links dynamic rainfall, LAC, and urban flood risk within a unified spatial analysis. Previous flood assessment studies have predominantly emphasized hydrological variables or flood hazard mapping without adequately considering the adaptive role of landscape characteristics in mitigating flood impacts (Cea & Costabile, 2022; Miranda et al., 2023). In contrast, the present study demonstrates that flood risk is not determined solely by rainfall variability but emerges from the interaction between hydrological forcing, urban exposure, and landscape resilience. The integration of dynamic rainfall analysis with LAC provides a more realistic representation of flood processes by simultaneously accounting for hazard generation, exposure, and ecological adaptation. Methodologically, this research contributes an integrated GIS-based framework capable of supporting multi-criteria flood risk assessment while offering a transferable approach applicable to rapidly urbanizing tropical cities experiencing increasing hydroclimatic variability. Consequently, the proposed framework advances current flood risk assessment methodologies by incorporating both environmental processes and ecosystem resilience into a single analytical model.

Beyond its scientific contribution, the findings have significant practical implications for sustainable urban planning and disaster risk reduction policies. The results indicate that improving LAC through the preservation of green open spaces, restoration of river corridors, enhancement of infiltration areas, and implementation of blue-green infrastructure can substantially reduce flood risk even under increasing rainfall intensity. Therefore, flood adaptation policies should move beyond conventional structural flood-control measures toward integrated Nature-Based Solutions that simultaneously strengthen ecosystem services and urban resilience (Liao, 2014; Fletcher et al., 2024; Hathaway et al., 2024; Liu & Zhang, 2025). Nevertheless, this study has several limitations. The analysis primarily considers dynamic rainfall and landscape characteristics without incorporating future climate change scenarios, socioeconomic dynamics, or real-time hydrodynamic simulations. Furthermore, the weighting of flood risk factors may vary depending on regional environmental conditions and data availability. Future studies are therefore recommended to integrate climate change projections, machine learning techniques, remote sensing time-series analysis, and hydrodynamic flood simulations to improve prediction accuracy and support adaptive flood management under future climatic uncertainty (He et al., 2026; Xiong & Yang, 2025). Overall, the conceptual model proposed in Figure 7 summarizes the scientific framework developed in this study and illustrates the interaction between dynamic rainfall, LAC, urban exposure, and integrated flood risk, thereby providing a comprehensive foundation for climate-resilient urban development.

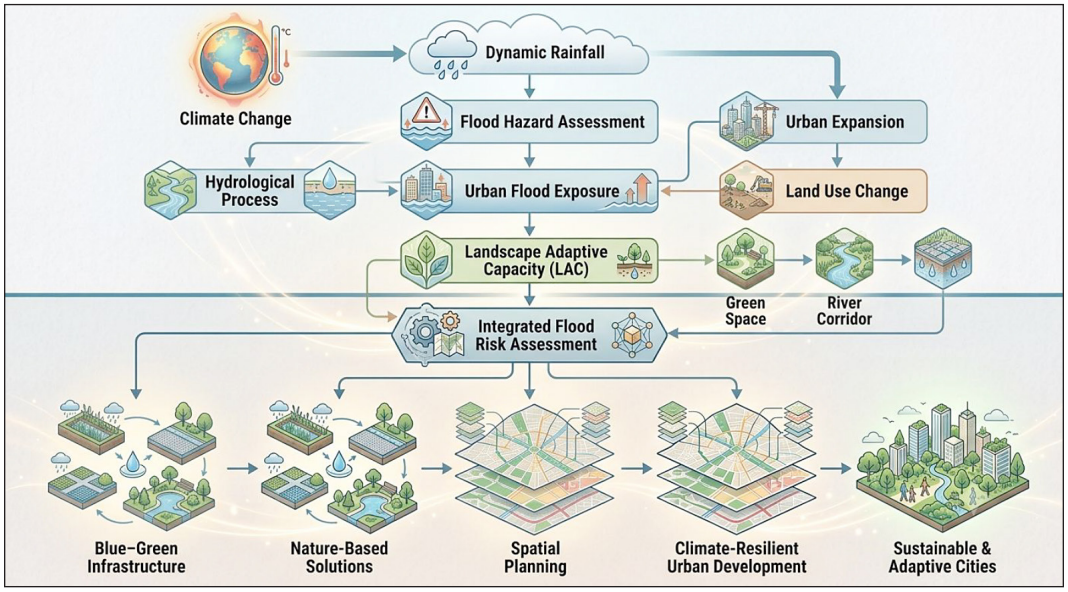

Figure 7. Conceptual framework of dynamic rainfall–landscape adaptive capacity–urban flood risk

Broader applicability and transferability of the PSAC framework

The proposed PSAC framework has potential applicability beyond Makassar City because its principal analytical structure is based on generally transferable components: temporal hydrological pressure, spatial flood susceptibility, urban exposure, and landscape adaptive-capacity indicators. The framework can therefore be adapted to other rapidly urbanizing tropical and coastal cities where rainfall variability, land-use transformation, flood susceptibility, and ecological capacity interact. Its transferability is strengthened by the use of GIS-based spatial operations, including data harmonization, spatial overlay, area calculation, indicator normalization, classification, and validation against available institutional or independent reference datasets. However, the framework should not be transferred mechanically without recalibration. The selection of indicators, classification thresholds, weights, spatial resolution, rainfall observation period, and definition of adaptive-capacity components should be adjusted according to local environmental conditions, data availability, administrative structures, and planning standards. For example, coastal cities may require additional consideration of tidal influence and sea-level conditions, while inland cities may place greater emphasis on river morphology, catchment response, or topographic controls. Similarly, cities with reliable event-based flood inventories may replace or supplement susceptibility-based validation with event-based predictive evaluation. Therefore, the broader applicability of the PSAC framework lies in its modular analytical structure rather than in the direct transfer of the numerical thresholds or results obtained for Makassar City. Future comparative applications across multiple cities would be necessary to test whether the framework produces consistent and transferable results under different hydroclimatic, urban, and institutional conditions.

CONCLUSIONS

This study developed and applied an integrated GIS-based framework combining dynamic rainfall analysis, flood hazard assessment, urban exposure analysis, and landscape adaptive capacity to evaluate spatial differences in urban flood-risk conditions. The quantitative results showed substantial rainfall variability during the 2015–2024 observation period, with monthly precipitation ranging from 42.7 to 612.4 mm and a coefficient of variation of 48.1%. The flood-hazard assessment classified 34.8% of the study area as high or very high hazard, while 28.6% was classified as moderate hazard. The exposure analysis showed that 41.2% of exposed assets were located within high and very high flood-hazard zones. Residential areas represented the largest exposed asset category, accounting for 34.6% of the total exposed assets, followed by road networks at 26.8%.

The LAC assessment classified 31.8% of the study area as having high to very high adaptive capacity and 29.6% as having low to very low adaptive capacity. Green open space covered 12.42% of the total urban area, which was 17.58 percentage points below the 30% spatial-planning benchmark used in this study. The integrated flood-risk assessment classified 24.7% of the study area as high or very high risk, whereas 35.9% was classified as low or very low risk. In the quantitative spatial validation, 9.83 km² of the 12.50 km² PSAC priority area overlapped with moderate-to-high BPBD flood-susceptibility areas, corresponding to a spatial overlap of 78.6%.

These quantitative results provide empirical evidence of substantial temporal rainfall variability, spatial differences in flood hazard, concentration of exposed assets in higher hazard zones, variation in landscape adaptive-capacity conditions, and substantial spatial agreement between PSAC priority areas and the official BPBD flood-susceptibility classification. The PSAC framework conceptually interprets these dimensions together as a basis for identifying areas where hydrological pressure, urban sensitivity, and landscape adaptive-capacity conditions occur in spatial proximity. This interpretation is conceptual and should not be understood as evidence of statistically estimated causal relationships among the individual dimensions.

The principal scientific contribution of this study is the empirical development and application of an integrated framework that links dynamic rainfall pressure, urban sensitivity, and LAC within a unified spatial assessment of urban flood risk. The framework does not claim to introduce entirely new individual analytical techniques; instead, its methodological contribution lies in systematically integrating established rainfall, GIS, exposure, susceptibility, and landscape-capacity analyses into a coherent PSAC assessment. The

new scientific knowledge generated by this integration is the quantitative demonstration that flood-priority areas can be distinguished according to the simultaneous occurrence of hydrological pressure, urban sensitivity, and limited adaptive landscape capacity. In the study area, this integrated interpretation is supported by substantial rainfall variability (CV = 48.1%), 34.8% of the area classified as high or very high flood hazard, 41.2% of exposed assets located within these hazard classes, limited GOS coverage of 12.42%, and a 78.6% spatial overlap between PSAC priority areas and moderate-to-high BPBD flood susceptibility. Therefore, the framework provides a scientifically structured approach for identifying spatial priorities for blue–green infrastructure, ecological restoration, land-use planning, and other adaptive interventions in tropical urban environments.

REFERENCES

1. Bilgiç, E., & Baba, A. (2023). Effect of urbanization on water resources: Challenges and prospects. In S. Ali & A. M. Armanuos (Eds.), *Groundwater in arid and semi-arid areas* (Earth and Environmental Sciences Library, pp. 81–108). Springer. https://doi.org/10.1007/978-3-031-43348-1_4.
2. Bishikwabo, I., Mambo, H., Kamanda, J. K., Abdelbaki, C., Nanyunga, M. A., & Kumar, N. (2025). Urban flood susceptibility mapping using GIS and Analytical Hierarchy Process: Case of City of Uvira, Democratic Republic of Congo. *GeoHazards, 6*(3), Article 38. https://doi.org/10.3390/geohazards6030038.
3. Cea, L., & Costabile, P. (2022). *Flood risk in urban areas: Modelling, management and adaptation to climate change. A review*. *Hydrology, 9*(3), Article 50. https://doi.org/10.3390/hydrology9030050.
4. Cruz, G., Vispo, C., Josue, M., Santos, F., & Briz, L. D. (2026). Influence of typhoon and monsoon-enhanced rainfall patterns on riverine flooding in Balanga City, Philippines. *Frontiers in Water, 8*, Article 1775842. https://doi.org/10.3389/frwa.2026.1775842.
5. Faccini, F., Luino, F., Paliaga, G., Roccati, A., & Turconi, L. (2021). Flash flood events along the West Mediterranean coasts: Inundations of urbanized areas conditioned by anthropic impacts. *Land, 10*(6), Article 620. https://doi.org/10.3390/land10060620.
6. Fletcher, T. D., Burns, M. J., Russell, K. L., Hamel, P., Duchesne, S., Cherqui, F., & Roy, A. H. (2024). Concepts and evolution of urban hydrology. *Nature Reviews Earth & Environment, 5*(11), 789–801. https://doi.org/10.1038/s43017-024-00599-x.
7. Guimarães, Y. C., Velastegui-Montoya, A., Carreiro, G. A., et al. (2026). Rainfall extremes and hydroclimatic trends in Caraguatatuba (SE Brazil) based on CHIRPS and ETCCDI indices (1981–2024). Theoretical and Applied Climatology, 157, Article 165. https://doi.org/10.1007/s00704-026-06094-1.
8. Hasbi, M. H. A., Lanuru, M., & Tumpu, M. (2025). Analysis of the availability of residential locations based on flood mitigation in Momunu District, Buol Regency. *Engineering, Technology & Applied Science Research, 15*(4), 25297–25303. https://doi.org/10.48084/etasr.10811.
9. Hathaway, J. M., Bean, E. Z., Bernagros, J. T., Christian, D. P., Davani, H., Ebrahimian, A., Fairbaugh, C. M., ... & Winston, R. J. (2024). A synthesis of climate change impacts on stormwater management systems: Designing for resiliency and future challenges. *Journal of Sustainable Water in the Built Environment, 10*(2), Article 03123004. https://doi.org/10.1061/JSWBAY.SWENG-533.
10. He, S., Neal, J., Lai, C., & Wang, Z. (2026). Explaining urban flood susceptibility under rainfall uncertainty through probabilistic modeling and interpretable machine learning. *Journal of Hydrology, 672*, Article 135430. https://doi.org/10.1016/j.jhydrol.2026.135430.
11. Ilmi, W. Z., Sunarharum, T. M., Santoso, H., Prihanto, Y., & Adinda, B. (2025). Tracing urban expansion and climate vulnerability through spatial-temporal indicators in a tropical coastal in Bandar Lampung City. *IOP Conference Series: Earth and Environmental Science, 1571*(1), Article 012015. https://doi.org/10.1088/1755-1315/1571/1/012015.
12. Kaiser, Z. R. M. A., & Akter, F. (2025). From risk to resilience and sustainability: Addressing urban flash floods and waterlogging. *Risk Sciences, 1*, Article 100011. https://doi.org/10.1016/j.risk.2025.100011.
13. Kumareswaran, K., & Jayasinghe, G. Y. (2023). *Green infrastructure and urban climate resilience: An introduction*. Springer. https://doi.org/10.1007/978-3-031-37081-6.
14. Latief, R., Budu, Tumpu, M., Hatta, M. P., & Aprianti, E. (2025). Quality of life analysis with WHOQOL-BREF in disaster preparedness for flood-prone areas in Makassar City, Indonesia. *Engineering, Technology & Applied Science Research, 15*(2), 22178–22186. https://doi.org/10.48084/etasr.10450.
15. Liao, K. H. (2014). From flood control to flood adaptation: A case study on the Lower Green River Valley and the City of Kent in King County, Washington. *Natural Hazards, 71*(1), 723–750. https://doi.org/10.1007/s11069-013-0923-4.
16. Liu, N., & Zhang, F. (2025). Urban green spaces and flood disaster management: Toward sustainable

urban design. *Frontiers in Public Health, 13*, Article 1583978. https://doi.org/10.3389/fpubh.2025.1583978.

17. McGrane, S. J. (2016). Impacts of urbanisation on hydrological and water quality dynamics, and urban water management: A review. *Hydrological Sciences Journal, 61*(13), 2295–2311. https://doi.org/10.1080/02626667.2015.1128084.
18. Miranda, F., Franco, A. B., Rezende, O., da Costa, B. B. F., Najjar, M., Haddad, A. N., & Miguez, M. (2023). A GIS-based index of physical susceptibility to flooding as a tool for flood risk management. *Land, 12*(7), Article 1408. https://doi.org/10.3390/land12071408.
19. Palacio-Aponte, A. G., Ortíz-Rodríguez, A. J., & Sandoval-Solis, S. (2022). Methodological framework for territorial planning of urban areas: Analysis of socio-economic vulnerability and risk associated with flash flood hazards. *Applied Geography, 149*, Article 102809. https://doi.org/10.1016/j.apgeog.2022.102809.
20. Posite, V. R., Ahana, B. S., Abdelbaki, C., Saber, M., Aliousseyni, L. Y., & Guadie, A. (2025). Multi-index detection of rainfall trends and climate shifts in urban tropical Kinshasa (1991–2023). *Results in Earth Sciences, 3*, Article 100106. https://doi.org/10.1016/j.rines.2025.100106.
21. Rahmawati, Tumpu, M., & Yunianta, A. (2025). Hydrodynamic and sedimentological impacts of intake gate opening adjustments for flood mitigation in water systems. *Engineering, Technology & Applied Science Research, 15*(4), 25438–25444. https://doi.org/10.48084/etasr.10729.
22. Ricart, S., Berizzi, C., Saurí, D., & Terlicher, G. N. (2022). The social, political, and environmental dimensions in designing urban public space from a water management perspective: Testing European experiences. *Land, 11*(9), Article 1575. https://doi.org/10.3390/land11091575.
23. Syahriwati, A., Muhiddin, A. H., Hatta, M. P., Aprianti, E., & Tumpu, M. (2025). HEC-RAS based modeling for the flood mitigation analysis of the Karema River. *Engineering, Technology & Applied Science Research, 15*(6), 29257–29262. https://doi.org/10.48084/etasr.12706.
24. Tang, J., Liu, D., Shang, C., & Niu, J. (2024). Impacts of land use change on surface infiltration capacity and urban flood risk in a representative karst mountain city over the last two decades. *Journal of Cleaner Production, 454*, Article 142196. https://doi.org/10.1016/j.jclepro.2024.142196.
25. Tumpu, M., Lanuru, M., Samawi, M. F., Assiddiqi, M. H., Kandou, C., Kabo, D. R. G., Tumengkol, H., Pinasang, D. B., Rachim, F., Yunianta, A., & Mansyur. (2026). Index-based spatial assessment of flood hazard and multi-sectoral vulnerability in flood-prone areas. *Civil Engineering and Architecture, 14*(1), 176–199. https://doi.org/10.13189/cea.2026.140112.
26. Wang, D., Xu, P.-Y., An, B.-W., & Guo, Q.-P. (2024). Urban green infrastructure: Bridging biodiversity conservation and sustainable urban development through adaptive management approach. *Frontiers in Ecology and Evolution, 12*, Article 1440477. https://doi.org/10.3389/fevo.2024.1440477.
27. Wang, Z., Chen, X., Qi, Z., & Cui, C. (2023). Flood sensitivity assessment of super cities. *Scientific Reports, 13*, Article 5582. https://doi.org/10.1038/s41598-023-32149-8.
28. Xing, Y., Liang, Q., Shao, D., & Ullah, I. (2025). Effects of urban topographical features on drainage efficiency for pluvial flash flood occurrence. *Natural Hazards, 121*(12), 14513–14529. https://doi.org/10.1007/s11069-025-07358-1.
29. Xiong, J., & Yang, Y. (2025). Climate change and hydrological extremes. *Current Climate Change Reports, 11*(1), Article 1. https://doi.org/10.1007/s40641-024-00198-4.
30. Yang, L. E., Scheffran, J., Süsser, D., Dawson, R., & Chen, Y. D. (2018). Assessment of flood losses with household responses: Agent-based simulation in an urban catchment area. *Environmental Modeling and Assessment, 23*(4), 369–388. https://doi.org/10.1007/s10666-018-9597-3.